cells among B220-positive cells in each HCV-Tg mouse. Bar graph indicates the percentage of cells with NF-κB p65 nuclear translocation in B220-positive cells. C: Bar graph shows the ratio of double-positive cells within the B220-positive cells in normal, asymptomatic and lymphomatous HCV-Tg mice. Ho: Hoechst33342 Data are presented as means ± S.E., * P<0.05, ** P<0.01, *** P<0.001. D: Western blot analysis: tissues from the spleen of controls (224-2, 3) or HCV-Tg mice without BCL (217-3, 224-4, 232-3) or with BCL (56-5, 69-5) were fractionated into nuclear and cytoplasmic fractions. NF-κB p50 and p65 were detected by antibodies. Relative ratios of quantitation by imager are indicated. GAPDH was detected as a loading control of the cytoplasmic fraction.
doi:10.1371/journal.pone.0091373.g004

Expression of A20 in HCV-associated BCL

In order to further validate the microarray results, we assessed A20 protein levels in BCLs isolated from HCV-Tg mice by Western blotting (Figure 3a). Two distinct anti-A20 antibodies recognising the N- (A20N) and C-terminal regions were used for the detection of A20. Regardless of the anti-A20 antibodies used, expression levels of A20 in BCL from HCV-Tg mice (Figure 3a, lanes 9 to 13) were markedly decreased when compared to splenocytes obtained from either BCL-non-developing HCV-negative mice (lanes 1 to 3) or from BCL-non-developing HCV-Tg mice (lanes 4 to 8). Quantitative analysis showed a significant decrease in A20 in BCLs obtained from HCV-Tg mice (Figure 3b). These results strongly suggest that the reduced expression of A20 is correlated with HCV-associated N-BHL development.

Nuclear localisation of NF-kB p65 in HCV-associated BCL

We next analysed the activation status of NF-κB by investigating the nuclear localisation of NF-κB p65 in cells positive for a B-cell marker molecule, B220, in BCLs isolated from HCV-Tg mice (Figure 4a). Quantitative analysis revealed that the ratio of cells double-positive for B220 and NF-κB p65 in the nuclei of the examined BCLs was significantly higher than the ratio in splenic tissue obtained from either BCL-non-developing HCV-negative mice or from BCL-non-developing HCV-Tg mice (Figures 4b and c). The fractionation assay showed that more NF-κB p50 and p65 were present in BCLs from HCV-Tg mice (Figure 4d). These results indicate the activation of NF-κB in HCV-associated BCL.

Expression of miR-26b in HCV-associated BCL

Recent studies have demonstrated that miR-26b is down-regulated in hepatocellular carcinoma [51], nasopharyngeal carcinoma [52], primary squamous cell lung carcinoma [53] and squamous cell carcinoma of the tongue [54]. In addition, miR-26b was down-regulated in HCV-positive SMZL when compared with HCV-negative counterparts [41] and in the PBMC of HCV-positive MC and NHL patients [42]. Therefore, we compared the expression levels of miR-26b in BCL from HCV-Tg mice with BCL from HCV-negative mice (i.e., spontaneously developed BCL) or in splenic tissue from BCL non-developing HCV-positive and -negative mice (Figure. 5). Interestingly, miR-26b expression was significantly down-regulated in BCLs from HCV-Tg mice. These results indicate that miR-26b is also down-regulated in HCV-associated BCL.

Discussion

In the present study, we identified differentially expressed genes in BCLs examined from HCV-Tg mice using a genome-wide microarray (Figures 1 and 2a, Table 1, and Figure S2). The microarray results for representative genes were validated at the RNA (Figures 2 and 5) and protein (Figures 3 and 4) levels. These findings helped dissect the molecular mechanisms underlying HCV-associated B-NHL development.

In the BCLs from HCV-Tg mice, the marked down-regulation of the Fos gene as well as other AP-1 protein genes (Fosb, Jun and Junb) was observed. Although AP-1 DNA binding activity was observed in Hodgkin-/multinuclear Reed-Sternberg cells and tissues from classical Hodgkin's disease, non-Hodgkin cell lines lacked the DNA binding activity of AP-1 [55]. Junb was weakly expressed in non-Hodgkin lymphomas of B-lymphoid origin; however, strong expression has been previously found in lymphomas that originated from the T-lymphoid lineage, and Junb selectively blocked B-lymphoid but not T-lymphoid cell proliferation ex vivo [56]. The BCL that developed in HCV-Tg mice was the non-Hodgkin type [43]; therefore, the decrease in AP-1 protein levels (Fos, Fosb, Jun, and Junb) may be crucial for lymphoma development.

In our previous study, soluble IL-2Rα levels were increased in BCL-developing HCV-Tg mice [43] Therefore, the up-regulation of IL-2Rα(Figure 2a) is potentially linked to the increase of soluble IL-2Rα, although further investigation is needed to clarify the details of this mechanism.

Expression of complement component C3 was significantly increased in BCLs isolated from HCV-Tg mice (Figure 2c). The presence of polymorphisms in complement system genes in non-Hodgkin lymphoma [57] suggests the involvement of complement in lymphoma development. The elevated C3 expression may be induced by TNF-α [58]. In addition, C3a, which is a cleavage product of C3, may contribute to the binding of NF-κB and AP-1 as shown previously [59].

The expression of LTβR, which is one of the key molecules in the alternative NF-κB signalling pathway [16], was significantly increased in BCLs from HCV-Tg mice (Figure 2d). HCV core proteins were reported to interact with the cytoplasmic domain of LTβR [60,61] and to enhance the alternative NF-κB signalling pathway [62]. The induction of LTβR by the HCV non-structural protein NS5B, and HCV RNA-dependent RNA polymerase, was also observed [63]. These findings suggest that the regulatory pathways involved in HCV infection also play a role in HCV-associated B-NHL development.

We observed several differences in the gene expression between male and female mice. Male HCV-negative mice showed up-regulation of LTβR and C3; however, female HCV-positive mice featured the downregulation of LTα and up-regulation of IL-2Rβ. Female HCV-Tg mice showed decreased overall survival in a previous study [43] and the above-mentioned gene dysregulations may contribute to this finding. However, the incidence of B-NHL between male and female mice did not show marked differences in the transgenic model [43]. Some clinical studies found gender-specific differences in the incidence of HCV-associated B-NHL and different effects of HCV on gene expression, which may also be dependent on gender [64]. However, meta-analyses did not provide consistent evidence for any gender preferences in HCV-NHL [48–50].

The down-regulation of A20, which is a ubiquitin-editing enzyme and tumour suppressor in various lymphomas [26], was observed in BCLs from HCV-Tg mice (Figures 3a and 3b). A20 has been reported to interact with the TNF receptor associated factor 2 (TRAF2), TRAF6, and the NF-κB essential modulator (NEMO). A20 inhibits NF-κB activation-induced by TNFα or by the overexpression of other proteins such as TRAF2 and receptor-interacting protein serine/threonine kinase 1 (RIPK1) proteins
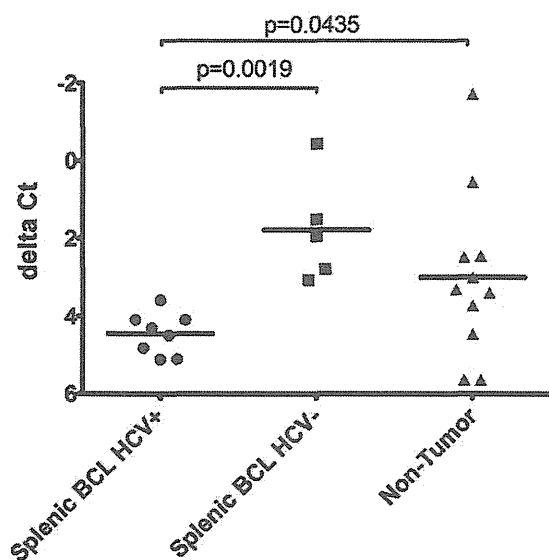
— 54 —

Figure 5. Quantification of miR-26b in BCL from HCV-positive and HCV-negative and non-tumour Tg mice. Formalin-fixed, paraffin-embedded (FFPE) splenic tissue from 24 animals (BCL HCV+, n = 8; BCL HCV-, n = 5; non-tumorous spleen HCV+/-, n = 11) was analysed for miR-26b expression by single assay stem-loop Q-RT-PCT by triplicate experiments. Data are shown as scatter dot-plots, and horizontal bar depicts the mean; y-axis: delta Ct (inverted scale) calculated in relation to endogenous control (snoRNA202). HCV-positive lymphoma tissue: filled circles; HCV-negative lymphoma tissue: filled squares; non-tumorous splenic tissue: filled triangles. P-values are shown in the graph.
doi:10.1371/journal.pone.0091373.g005

[65]. RIPK3 contributes to TNFR1-mediated RIPK1-dependent apoptosis and necroptosis [66]. RIPK2 (also known as RIP2) is also involved in B cell lymphoma cell survival and mediates the activation of NF-κB and MAPK pathways, associated with the TNF receptor family [67]. Therefore, suppression of A20 activates NF-κB by increasing nuclear translocation in tumour tissues.

Expression of miR-26b in BCLs obtained from HCV-Tg mice was significantly down-regulated (Figure 5). miR-26b is also down-regulated in numerous cancers, e.g., HCC [51], nasopharyngeal carcinomas [52], primary squamous cell lung carcinomas [53]and squamous cell carcinoma tongue [54]. In addition, c-Myc, which is up-regulated in various cancer types, has been shown to contribute to the reduction of miR-26a/b expression [68]. Notably, expression of miR-26b was significantly down-regulated in SMZL arising in HCV-positive patients [41]. Although the mechanisms

of miR-26b-mediated tumourigenicity regulation are not fully understood, previous reports [69] and the present study have suggested a possible regulatory role of miR-26b in HCV-related lymphoma. Several candidates are reported to be targets of miR-26b. miR-26a and miR-26b are regulators of EZH2, which is the PRC2 polycomb repressive complex, is overexpressed in multiple cancers and is a target of the MYC oncogene [70]. In addition, lymphoid enhancer factor (LEF)-1 [42] and Nek6 [41] are targets of miR-26b. LEF-1 is a nuclear transcription factor that forms a complex with β-catenine and T-cell factor and induces transcription of cyclin D1 and c-myc. Nek6 is a kinase involved in the initiation of mitosis and is overexpressed in various tumours. The phosphatase and tensin homolog gene (PTEN) is also the putative target gene of miR-26b in adipogenic regulation [71] and cell growth [72].

This report is the first to demonstrate the possible involvement of networks of NF-κB, AP-1, complements and miR-26b in HCV-associated B-NHL (Figure S2). A future study focusing on the dysregulation of these networks and their modification by HCV may provide valuable information on improving therapy for HCV-associated B-NHL.

Supporting Information

Figure S1 A: B cells were isolated from mice using MACS beads and anti-CD19 antibody. The population of B cells was confirmed by staining with anti-B220 antibody. **B:** RNA integrity number (RIN) was measured using an Agilent 2100 Bioanalyzer (Agilent) for the estimation of purity.
(PDF)

Figure S2 Possible pathways involved in BCL development. Both canonical and alternative NF-κB pathways may play a role. Bold arrows indicate up-regulation or down-regulation. NIK; NF-κB-inducing kinase.
(PDF)

Acknowledgments

Author Contributions

Conceived and designed the experiments: KT-K T. Mizuochi. Performed the experiments: YK T. Mizukami HK JP-O KT-K. Analyzed the data: YN JP-O T. Mizuochi KT-K. Contributed reagents/materials/analysis tools: MK. Wrote the paper: MO JP-O T. Mizuochi KT-K.

References

1. Shepard CW, Finelli L, Alter MJ (2005) Global epidemiology of hepatitis C virus infection. Lancet Infect Dis 5: 558–567.
2. Libra M, Gasparotto D, Gloghini A, Navolanic PM, De Re V, et al. (2005) Hepatitis C virus (HCV) I hepatitis C virus (HCV) infection and lymphoproliferative disorders. Front Biosci 10: 2460–2471.
3. Saito I, Miyamura T, Ohbayashi A, Harada H, Katayama T, et al. (1990) Hepatitis C virus infection is associated with the development of hepatocellular carcinoma. Proc Natl Acad Sci U S A 87: 6547–6549.
4. Silvestri F, Pipan C, Barillari G, Zaja F, Fanin R, et al. (1996) Prevalence of hepatitis C virus infection in patients with lymphoproliferative disorders. Blood 87: 4296–4301.
5. Ascoli V, Lo Coco F, Artini M, Levrero M, Martelli M, et al. (1998) Extranodal lymphomas associated with hepatitis C virus infection. Am J Clin Pathol 109: 600–609.
6. Mele A, Pulsoni A, Bianco E, Musto P, Szklo A, et al. (2003) Hepatitis C virus and B-cell non-Hodgkin lymphomas: an Italian multicenter case-control study. Blood 102: 996–999.

7. Ito M, Kusunoki H, Mizuochi T (2011) Peripheral B cells as reservoirs for persistent HCV infection. Front Microbiol 2: 177.
8. Dammacco F, Sansonno D, Piccoli C, Racanelli V, D'Amore FP, et al. (2000) The lymphoid system in hepatitis C virus infection: autoimmunity, mixed cryoglobulinemia, and Overt B-cell malignancy. Semin Liver Dis 20: 143–157.
9. Peveling-Oberhag J, Arcaini L, Hansmann ML, Zeuzem S (2013) Hepatitis C-associated B-cell non-Hodgkin lymphomas. Epidemiology, molecular signature and clinical management. J Hepatol 59: 169–177.
10. Hermine O, Lefrere F, Bronowicki JP, Mariette X, Jondeau K, et al. (2002) Regression of splenic lymphoma with villous lymphocytes after treatment of hepatitis C virus infection. N Engl J Med 347: 89–94.
11. Hess J, Angel P, Schorpp-Kistner M (2004) AP-1 subunits: quarrel and harmony among siblings. J Cell Sci 117: 5965–5973.
12. Vasanwala FH, Kusam S, Toney LM, Dent AL (2002) Repression of AP-1 function: a mechanism for the regulation of Blimp-1 expression and B lymphocyte differentiation by the B cell lymphoma-6 protooncogene. J Immunol 169: 1922–1929.

— 55 —

13. Pekarsky Y, Palamarchuk A, Maximov V, Efanov A, Nazaryan N, et al. (2008) Tcl1 functions as a transcriptional regulator and is directly involved in the pathogenesis of CLL. Proc Natl Acad Sci U S A 105: 19643–19648.

14. Ghosh S, Karin M (2002) Missing pieces in the NF-kappaB puzzle. Cell 109 Suppl: S81–96.

15. Sen R, Baltimore D (1986) Inducibility of kappa immunoglobulin enhancer-binding protein Nf-kappa B by a posttranslational mechanism. Cell 47: 921–928.

16. Bakkar N, Guttridge DC (2010) NF-kappaB signaling: a tale of two pathways in skeletal myogenesis. Physiol Rev 90: 495–511.

17. Sun B, Karin M (2008) NF-kappaB signaling, liver disease and hepatoprotective agents. Oncogene 27: 6228–6244.

18. Arsura M, Cavin LG (2005) Nuclear factor-kappaB and liver carcinogenesis. Cancer Lett 229: 157–169.

19. Haybaeck J, Zeller N, Wolf MJ, Weber A, Wagner U, et al. (2009) A lymphotoxin-driven pathway to hepatocellular carcinoma. Cancer Cell 16: 295–308.

20. De Re V, Caggiari L, Garziera M, De Zorzi M, Repetto O (2012) Molecular signature in HCV-positive lymphomas. Clin Dev Immunol 2012: 623465.

21. Opipari AW, Jr., Boguski MS, Dixit VM (1990) The A20 cDNA induced by tumor necrosis factor alpha encodes a novel type of zinc finger protein. J Biol Chem 265: 14705–14708.

22. Song HY, Rothe M, Goeddel DV (1996) The tumor necrosis factor-inducible zinc finger protein A20 interacts with TRAF1/TRAF2 and inhibits NF-kappaB activation. Proc Natl Acad Sci U S A 93: 6721–6725.

23. Lee EG, Boone DL, Chai S, Libby SL, Chien M, et al. (2000) Failure to regulate TNF-induced NF-kappaB and cell death responses in A20-deficient mice. Science 289: 2350–2354.

24. Heyninck K, Beyaert R (2005) A20 inhibits NF-kappaB activation by dual ubiquitin-editing functions. Trends Biochem Sci 30: 1–4.

25. Malynn BA, Ma A (2009) A20 takes on tumors: tumor suppression by an ubiquitin-editing enzyme. J Exp Med 206: 977–980.

26. Hymowitz SG, Wertz IE (2010) A20: from ubiquitin editing to tumour suppression. Nat Rev Cancer 10: 332–341.

27. Kato M, Sanada M, Kato I, Sato Y, Takita J, et al. (2009) Frequent inactivation of A20 in B-cell lymphomas. Nature 459: 712–716.

28. Honma K, Tsuzuki S, Nakagawa M, Karnan S, Aizawa Y, et al. (2008) TNFAIP3 is the target gene of chromosome band 6q23.3-q24.1 loss in ocular adnexal marginal zone B cell lymphoma. Genes Chromosomes Cancer 47: 1–7.

29. Honma K, Tsuzuki S, Nakagawa M, Tagawa H, Nakamura S, et al. (2009) TNFAIP3/A20 functions as a novel tumor suppressor gene in several subtypes of non-Hodgkin lymphomas. Blood 114: 2467–2475.

30. Schmitz R, Hansmann ML, Bohle V, Martin-Subero JI, Hartmann S, et al. (2009) TNFAIP3 (A20) is a tumor suppressor gene in Hodgkin lymphoma and primary mediastinal B cell lymphoma. J Exp Med 206: 981–989.

31. Compagno M, Lim WK, Grunn A, Nandula SV, Brahmachary M, et al. (2009) Mutations of multiple genes cause deregulation of NF-kappaB in diffuse large B-cell lymphoma. Nature 459: 717–721.

32. Parvatiyar K, Barber GN, Harhaj EW (2010) TAX1BP1 and A20 inhibit antiviral signaling by targeting TBK1-IKKi kinases. J Biol Chem 285: 14999–15009.

33. Parvatiyar K, Harhaj EW (2011) Regulation of inflammatory and antiviral signaling by A20. Microbes Infect 13: 209–215.

34. Tavares RM, Turer EE, Liu CL, Advincula R, Scapini P, et al. (2010) The ubiquitin modifying enzyme A20 restricts B cell survival and prevents autoimmunity. Immunity 33: 181–191.

35. Verstrepen L, Verhelst K, van Loo G, Carpentier I, Ley SC, et al. (2010) Expression, biological activities and mechanisms of action of A20 (TNFAIP3). Biochem Pharmacol 80: 2009–2020.

36. He L, Hannon GJ (2004) MicroRNAs: small RNAs with a big role in gene regulation. Nat Rev Genet 5: 522–531.

37. Lawrie CH (2007) MicroRNA expression in lymphoma. Expert Opin Biol Ther 7: 1363–1374.

38. Jopling CL, Yi M, Lancaster AM, Lemon SM, Sarnow P (2005) Modulation of hepatitis C virus RNA abundance by a liver-specific MicroRNA. Science 309: 1577–1581.

39. Kim SW, Ramasamy K, Bouamar H, Lin AP, Jiang D, et al. (2012) MicroRNAs miR-125a and miR-125b constitutively activate the NF-kappaB pathway by targeting the tumor necrosis factor alpha-induced protein 3 (TNFAIP3, A20). Proc Natl Acad Sci U S A 109: 7865–7870.

40. Hother C, Rasmussen PK, Joshi T, Reker D, Ralfkiaer U, et al. (2013) MicroRNA Profiling in Ocular Adnexal Lymphoma: A Role for MYC and NFKB1 Mediated Dysregulation of MicroRNA Expression in Aggressive Disease. Invest Ophthalmol Vis Sci 54: 5169–5175.

41. Peveling-Oberhag J, Crisman G, Schmidt A, Doring C, Lucioni M, et al. (2012) Dysregulation of global microRNA expression in splenic marginal zone lymphoma and influence of chronic hepatitis C virus infection. Leukemia 26: 1654–1662.

42. Fognani E, Giannini C, Piluso A, Gragnani L, Monti M, et al. (2013) Role of microRNA profile modifications in hepatitis C virus-related mixed cryoglobulinemia. PLoS One 8: e62965.

43. Kasama Y, Sekiguchi S, Saito M, Tanaka K, Satoh M, et al. (2010) Persistent expression of the full genome of hepatitis C virus in B cells induces spontaneous development of B-cell lymphomas in vivo. Blood 116: 4926–4933.

44. Tsukiyama-Kohara K, Tone S, Maruyama I, Inoue K, Katsume A, et al. (2004) Activation of the CKI-CDK-Rb-E2F pathway in full genome hepatitis C virus-expressing cells. J Biol Chem 279: 14531–14541.

45. Rickert RC, Roes J, Rajewsky K (1997) B lymphocyte-specific, Cre-mediated mutagenesis in mice. Nucleic Acids Res 25: 1317–1318.

46. Nishimura T, Kohara M, Izumi K, Kasama Y, Hirata Y, et al. (2009) Hepatitis C virus impairs p53 via persistent overexpression of 3beta-hydroxysterol Delta24-reductase. J Biol Chem 284: 36442–36452.

47. Yamazaki J, Mizukami T, Takizawa K, Kuramitsu M, Momose H, et al. (2009) Identification of cancer stem cells in a Tax-transgenic (Tax-Tg) mouse model of adult T-cell leukemia/lymphoma. Blood 114: 2709–2720.

48. Gisbert JP, Garcia-Buey L, Pajares JM, Moreno-Otero R (2003) Prevalence of hepatitis C virus infection in B-cell non-Hodgkin's lymphoma: systematic review and meta-analysis. Gastroenterology 125: 1723–1732.

49. Matsuo K, Kusano A, Sugumar A, Nakamura S, Tajima K, et al. (2004) Effect of hepatitis C virus infection on the risk of non-Hodgkin's lymphoma: a meta-analysis of epidemiological studies. Cancer Sci 95: 745–752.

50. de Sanjose S, Benavente Y, Vajdic CM, Engels EA, Morton LM, et al. (2008) Hepatitis C and non-Hodgkin lymphoma among 4784 cases and 6269 controls from the International Lymphoma Epidemiology Consortium. Clin Gastroenterol Hepatol 6: 451–458.

51. Ji J, Shi J, Budhu A, Yu Z, Forgues M, et al. (2009) MicroRNA expression, survival, and response to interferon in liver cancer. N Engl J Med 361: 1437–1447.

52. Ji Y, He Y, Liu L, Zhong X (2010) MiRNA-26b regulates the expression of cyclooxygenase-2 in desferrioxamine-treated CNE cells. FEBS Lett 584: 961–967.

53. Gao W, Shen H, Liu L, Xu J, Xu J, et al. (2011) MiR-21 overexpression in human primary squamous cell lung carcinoma is associated with poor patient prognosis. J Cancer Res Clin Oncol 137: 557–566.

54. Wong TS, Liu XB, Wong BY, Ng RW, Yuen AP, et al. (2008) Mature miR-184 as Potential Oncogenic microRNA of Squamous Cell Carcinoma of Tongue. Clin Cancer Res 14: 2588–2592.

55. Mathas S, Hinz M, Anagnostopoulos I, Krappmann D, Lietz A, et al. (2002) Aberrantly expressed c-Jun and JunB are a hallmark of Hodgkin lymphoma cells, stimulate proliferation and synergize with NF-kappa B. EMBO J 21: 4104–4113.

56. Szremska AP, Kenner L, Weisz E, Ott RG, Passegue E, et al. (2003) JunB inhibits proliferation and transformation in B-lymphoid cells. Blood 102: 4159–4165.

57. Bassig BA, Zheng T, Zhang Y, Berndt SI, Holford TR, et al. (2012) Polymorphisms in complement system genes and risk of non-Hodgkin lymphoma. Environ Mol Mutagen 53: 145–151.

58. Andoh A, Fujiyama Y, Hata K, Araki Y, Takaya H, et al. (1999) Counter-regulatory effect of sodium butyrate on tumour necrosis factor-alpha (TNF-alpha)-induced complement C3 and factor B biosynthesis in human intestinal epithelial cells. Clin Exp Immunol 118: 23–29.

59. Fischer WH, Jagels MA, Hugli TE (1999) Regulation of IL-6 synthesis in human peripheral blood mononuclear cells by C3a and C3a(desArg). J Immunol 162: 453–459.

60. Matsumoto M, Hsieh TY, Zhu N, VanArsdale T, Hwang SB, et al. (1997) Hepatitis C virus core protein interacts with the cytoplasmic tail of lymphotoxin-beta receptor. J Virol 71: 1301–1309.

61. Chen CM, You LR, Hwang LH, Lee YH (1997) Direct interaction of hepatitis C virus core protein with the cellular lymphotoxin-beta receptor modulates the signal pathway of the lymphotoxin-beta receptor. J Virol 71: 9417–9426.

62. You LR, Chen CM, Lee YH (1999) Hepatitis C virus core protein enhances NF-kappaB signal pathway triggering by lymphotoxin-beta receptor ligand and tumor necrosis factor alpha. J Virol 73: 1672–1681.

63. Simonin Y, Vegna S, Akkari L, Gregoire D, Antoine E, et al. (2013) Lymphotoxin Signaling Is Initiated by the Viral Polymerase in HCV-linked Tumorigenesis. PLoS Pathog 9: e1003234.

64. Vladareanu AM, Ciufu C, Neagu AM, Onisai M, Bumbea H, et al. (2010) The impact of hepatitis viruses on chronic lymphoproliferative disorders—preliminary results. J Med Life 3: 320–329.

65. Heyninck K, De Valck D, Vanden Berghe W, Van Criekinge W, Contreras R, et al. (1999) The zinc finger protein A20 inhibits TNF-induced NF-kappaB-dependent gene expression by interfering with an RIP- or TRAF2-mediated transactivation signal and directly binds to a novel NF-kappaB-inhibiting protein ABIN. J Cell Biol 145: 1471–1482.

66. Dondelinger Y, Aguileta MA, Goossens V, Dubuisson C, Grootjans S, et al. (2013) RIPK3 contributes to TNFR1-mediated RIPK1 kinase-dependent apoptosis in conditions of cIAP1/2 depletion or TAK1 kinase inhibition. Cell Death Differ 20: 1381–1392.

67. Cai X, Du J, Liu Y, Xia W, Liu J, et al. (2013) Identification and characterization of receptor-interacting protein 2 as a TNFR-associated factor 3 binding partner. Gene 517: 205–211.

68. Zhu Y, Lu Y, Zhang Q, Liu JJ, Li TJ, et al. (2012) MicroRNA-26a/b and their host genes cooperate to inhibit the G1/S transition by activating the pRb protein. Nucleic Acids Res 40: 4615–4625.

69. Ma YL, Zhang P, Wang F, Moyer MP, Yang JJ, et al. (2011) Human embryonic stem cells and metastatic colorectal cancer cells shared the common endogenous human microRNA-26b. J Cell Mol Med 15: 1941–1954.

— 56 —

70. Koh CM, Iwata T, Zheng Q, Bethel C, Yegnasubramanian S, et al. (2011) Myc enforces overexpression of EZH2 in early prostatic neoplasia via transcriptional and post-transcriptional mechanisms. Oncotarget 2: 669–683.

71. Song G, Xu G, Ji C, Shi C, Shen Y, et al. (2014) The role of microRNA-26b in human adipocyte differentiation and proliferation. Gene 533: 481–487.

72. Palumbo T, Faucz FR, Azevedo M, Xekouki P, Iliopoulos D, et al. (2013) Functional screen analysis reveals miR-26b and miR-128 as central regulators of pituitary somatomammotrophic tumor growth through activation of the PTEN-AKT pathway. Oncogene 32: 1651–1659.

73. Tsukiyama-Kohara K, Poulin F, Kohara M, DeMaria CT, Cheng A, et al. (2001) Adipose tissue reduction in mice lacking the translational inhibitor 4E-BP1. Nat Med 7: 1128–1132.

副反応に対する情報収集と迅速な対応
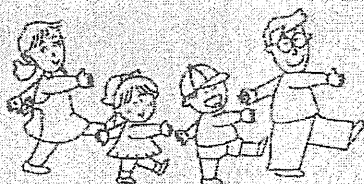
国立感染症研究所感染症疫学センター　多屋馨子

はじめに

予防接種は"ワクチン"という薬剤を接種する医療行為のことで，感染症予防のために最も特異的で，かつ効果の高い方法です。ワクチンの有効性と安全性については，さまざまな方法で検討が行われています。ヒトを対象とした臨床治験が終了すると，その結果をもとに，さまざまな観点からの審査が行われます。これらの審査の結果，薬事法という法律に基づいて製造販売承認がなされると，国立感染症研究所で国家検定が行われます。日本では，市場に流通しているのは国家検定に合格したワクチンのみとなっています（医師が海外から個人輸入したワクチンについては，国家検定は行われていません）。

このようにさまざまな観点から丁寧に有効性・安全性が確認されて，

実際に子どもたちに接種が行われることになるのですが，詳細な検討にもかかわらず，まれながら予防接種後に好ましくない症状が現れることがあります。

薬剤の投与後に起こった好ましくない症状を"副作用"といいますが，ワクチンの場合は，薬の"作用"を期待しているのではなく，予防接種を受けた者の免疫反応を期待していることから，ワクチンによって起こった好ましくない反応を"副反応"とよびます。副反応を完全に"ゼロ"にすることは困難で，一定頻度で副反応は発生します。そのため，「ワクチンによる副反応，あるいは副反応が否定できない」と認定された場合は，健康被害救済制度があります。もし健康被害救済を申請する場合は，副反応報告とは別の書類を提出する必要があります。

"有害事象"と"副反応"はどう違うの？

予防接種後に起こった好ましくない症状が，ワクチンによるものか，あるいは別の原因によって偶然予防接種後に起こったものかの区別は，ときに難しい場合があります。そのため，因果関係にかかわらず，接種後に起こった好ましくない症状を"有害事象"とよび，厚生労働省は医療機関や製造販売会社等に報告を求めています。

"有害事象"の中で，ワクチンとの因果関係があると判断されたものを"副反応"といいます。偶然にも予防接種後に別の原因によって好ましくない症状が現れる場合がありますが，これを"紛れ込み"といいます。

以上のことを理解したうえで，予防接種後に，これまで想定されていなかった異常な副反応が発生してい

著者プロフィール　1986年高知医科大学（現 高知大学医学部医学科）卒業。大阪大学医学部小児科学講座入局。大阪市立小児保健センター，大阪市立桃山病院感染症センター，大阪市立城北市民病院，大阪大学医学部附属病院で研修医，勤務医の後，1994年大阪大学医学部微生物学講座助手，1996年大阪大学医学部小児科学講座助手を経て，2001年から国立感染症研究所感染症情報センター主任研究官，2002年から国立感染症研究所感染症情報センター室長。なお，2013年4月に名称が国立感染症研究所感染症疫学センターに変更。

(a)

(b)

図1 予防接種後副反応報告書（医療機関用）
(a) 1枚目。 (b) 2枚目。 2014年10月1日から定期接種に導入される水痘ワクチンと高齢者の肺炎球菌ワクチンが入った新しい報告書。
[http://www.mhlw.go.jp/topics/bcg/tp250330-1.html]

ないか，これまで報告されていた副反応であっても，通常想定される頻度を超えて発生していないか，年齢，接種時期，接種医療機関，ワクチンの種類，ロット番号等に集積がみられないかをサーベイランスすることはとても大切です。早期に異常を探知して迅速な対策をとることが，国民の安心・安全に繋がります。

副反応に対する情報収集はどのように行われているの？

2013年3月に予防接種法が一部改正され（平成25年法律8号），同年4月1日から病院もしくは診療所の開設者または医師に「予防接種後副反応報告」が義務づけられました。

また，薬局開設者，病院もしくは診療所の開設者または医師，歯科医師，薬剤師その他医薬関係者は，

著者連絡先 〒162-8640 東京都新宿区戸山1-23-1 国立感染症研究所感染症疫学センター

「死亡」「障害」「死亡につながるおそれのあるもの」「障害につながるおそれのあるもの」「治療のために病院または診療所への入院または入院期間の延長が必要とされる症状を認めたもの」「上記に準じて重篤であるもの」「後世代における先天性の疾病または異常」等を認めた場合は，薬事法第77条の4の2に基づき，報告が義務づけられています。

これまで複雑であった報告様式は簡略化され，定期接種・任意接種の区別なく，同じ様式で報告できることになりました。また，法令で定められた症状が予防接種後の一定期間の間に発生した場合は，予防接種との因果関係にかかわらず，厚生労働省に直接FAXで報告することが医療機関に義務づけられました（図1(a)および図1(b)）。すなわち「有害事象報告」が正確な表現になります。

一方，図1(b)に記載されていない症状であっても，①入院 ②死亡または永続的な機能不全に陥るまたは陥る恐れがある場合であって，それが予防接種を受けたことによるものと疑われる症状については，「その他の反応」として報告が求められています。図1(a)および図1(b)の電子媒体は，厚生労働省のホームページに公開されており，PDF版，エクセル版の両方でダウンロード可能となっています。

また，医療機関が図1(a)および図1(b)に基づいて厚生労働省に報告すれば，薬事法に基づく報告も兼

ねることになりました。2013年3月まで，定期接種は実施主体である市区町村に，任意接種は独立行政法人医薬品医療機器総合機構（以下，PMDAという）に副反応報告がなされていましたが，医療機関から厚生労働省へのFAX（FAX番号：0120-510-355）による直接報告になり，市区町村へは，厚生労働省から都道府県を通じて速やかに情報還元されることになりました（図2）。

また，被接種者や保護者からも報告ができるように，保護者用の副反

応報告様式が定められました（図3）。

迅速な対応をどのように行っていくか

厚生労働省に届けられた副反応報告を解析し，異常な集積が認められた場合や，重篤な副反応が報告された場合は，厚生労働省，国立感染症研究所，PMDAは協力・連携して副反応報告を解析し，情報を整理し，調査を実施する等，迅速な対応を行うことになっています。また，整理

副反応報告制度
○予防接種制度上の副反応報告と薬事制度上の副作用等報告を厚生労働省に一元化し，医療機関の報告事務を簡素化。
○報告を受けた副反応報告の個別事例について，厚生労働省が(独)医薬品医療機器総合機構に情報整理及び調査を委託。
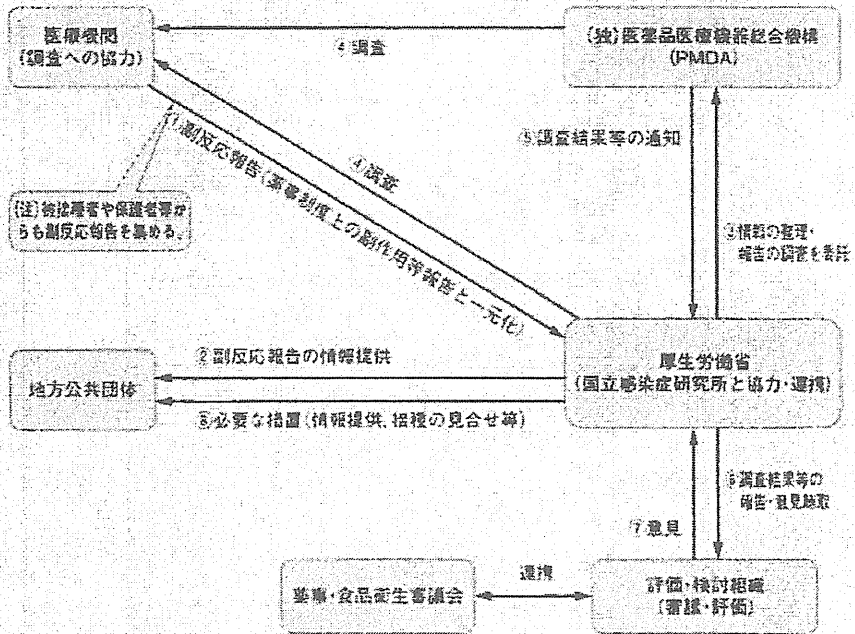○厚生科学審議会が薬事・食品衛生審議会と連携して副反応報告に係る評価を行ったうえで，厚生労働省が必要な措置を行う。

図2　予防接種後副反応報告の流れ
[第1回予防接種・ワクチン分科会副反応検討部会配付資料（平成25年5月16日）]

図3 予防接種後副反応報告書（保護者報告用）
(http://www.mhlw.go.jp/bunya/kenkou/kekkaku-kansenshou20/dl_yobou130417-2.pdf)

おわりに

　副反応報告を行いやすい体制づくりに加えて，副反応の集積が認められた場合は，迅速にそれを探知する仕組みを構築していくことが，今後必要です。また，接種者数をリアルタイムに把握して，分母情報が迅速に得られるようにすることも，副反応の頻度を検討するうえで，きわめて重要です。

　まれながら認められる重篤な副反応については，一例一例の丁寧な調査に加えて，積極的疫学調査が今後必要になってくると考えています。

◆参考文献◆
・多屋馨子：副反応報告と救済制度，公衆衛生 78（2）：86-92，2014
・多屋馨子：副反応報告制度，小児科 54（12）：1615-1630，2013
・多屋馨子：副反応・有害事象報告制度はどう変わったか，小児科臨床 66（9）：1859-1869，2013
・多屋馨子：予防接種健康被害救済制度・予防接種後副反応・健康状況調査，小児科診療 72（12）：2241-2250，2009
・多屋馨子：予防接種後副反応・健康状況調査，母子保健情報 59：42-48，2009
・加藤達夫，岡田賢司，庵原俊昭，ほか：予防接種と副反応，小児保健研究 65（5）：698-699，2006
・多屋馨子：定期接種　副反応，小児看護 27（12）：1609-1615，2004

した情報は，厚生科学審議会予防接種・ワクチン分科会副反応検討部会，薬事・食品衛生審議会医薬品等安全対策部会安全対策調査会の合同開催により定期的に検討がなされ，

資料については厚生労働省のホームページに公表されています（http://www.mhlw.go.jp/stf/shingi/2r98520000008f2q.html#shingi127715）。

Degenerate polymerase chain reaction strategy with DNA microarray for detection of multiple and various subtypes of virus during blood screening

Kazuya Takizawa,* Tatsuo Nakashima,* Takuo Mizukami,* Madoka Kuramitsu, Daiji Endoh, Shigeto Kawauchi, Kohsuke Sasaki, Haruka Momose, Yoshiharu Kiba, Tetsuya Mizutani, Rika A. Furuta, Kazunari Yamaguchi, and Isao Hamaguchi

BACKGROUND: The risk of transferring blood-borne infections during transfusion is continually increasing because of newly emerging and reemerging viruses. Development of a rapid screening method for emerging viruses that might be transmitted by transfusion is required to eliminate such pathogens during blood donor screening. Owing to increased use of human materials in organ transplants and cell therapy, the risk of donor-transmitted viral infections is also increasing. Although nucleic acid amplification technology (NAT) is dedicated to blood screening, a small, convenient detection system is needed at the laboratory and hospital level.

STUDY DESIGN AND METHODS: We developed a new pathogen detection system that can detect multiple viruses simultaneously, using originally designed degenerate polymerase chain reaction primers to amplify a wide range of viral genotypes. Amplified samples were identified using a DNA microarray of pathogen-specific probes.

RESULTS: We detected very low copy numbers of multiple subtypes of viruses, such as human hepatitis C virus (HCV), human hepatitis B virus (HBV), human parvovirus B19 (PVB19), and West Nile virus (WNV), using a single plate. We also detected all genotypes of human immunodeficiency virus (HIV) but sensitivity was less than for the other viruses.

CONCLUSION: We developed a microarray assay using novel primers for detection of a wide range of multiple pathogens and subtypes. Our NAT system was accurate and reliable for detection of HIV, HBV, HCV, PVB19, and WNV, with respect to specificity, sensitivity, and genotype inclusivity. Our system could be customized and extended for emerging pathogens and is suitable as a future NAT system.

Quality and safety in blood products are major public health concerns. In addition to general quality control (QC) testing, introduction of good manufacturing practice and routine screening of blood material and products have assured consistency and quality in production and increased blood transfusion safety in recent decades. Newly developed serologic tests and nucleic acid technology (NAT) have markedly reduced the risk of transmitting human immunodeficiency virus (HIV), hepatitis C virus (HCV), and hepatitis B virus (HBV) from infected blood.[1] Currently, several Food and Drug Administration (FDA)-licensed NAT assays are available to screen blood donors for HIV, HCV, HBV, and West Nile virus (WNV). However,

TABLE 1. Pathogen-specific dPCR primers for microarray detection*					
Pathogens	Primer sequence (5'-3')	GenBank Accession Number	Position (NT)	Gene name	Amplicons (bp)
HIV	RARAGGGGGGATTGGGGGGTA YTGTCYCTGWAATAAACCCGA	NC_001802	4336-4356 4444-4464	Integrase	129
HCV	GAAAGCGYCTAGCCATGGCGT TGCACGGTCTACGAGACCTCC	D90208	59-327 307-327	5'-UTR	269
HBV	AYTAYCAAGGTATGTTGCCCG GGAAAGCCCKRCGMACCACTG	X70185	450-470 695-715	S	266
PVB19	AGTGGTGGTGAAAGCTCTGAA TCTCCTGAACTGGTCCCG	NC_000883	2148-2168 2252-2269	NS1	122
WNV	GGHTGTTGGTATGGNATGGA CTCCTGGGTGRCCAAGAAC	NC_009942	3451-3590 3573-3591	NS1 NS2A	141
IC	TCGAAGACGATCAGATACCGT ATACTCCCCCCGGAACC	M10098	1147-1157 1259-1275	18S rRNA	129

* Code base description: M, A/C; R, A/G; W, A/T; S, C/G; Y, C/T; K, G/T; V, A/C/G; H, A/C/T; D, A/G/T; B, C/G/T; N, A/T/C/G.

the continuous development of a highly sensitive screening system is a challenging task for NAT. The focus is mainly on assay sensitivity rather than the range and diversity of viral species detected; therefore, the current NAT systems only ensure detection of a restricted range of viruses and their subtypes and not newly diverged, emerging, or reemerging viruses.[2] It has been reported that the NAT sensitivity for HCV detection differs slightly in relation to virus subtype.[3] Recent advances in organ transplantation and cell therapy have also increased the risk of donor-transmitted viral infections, such as cytomegalovirus, Epstein–Barr virus, WNV, and lymphocytic choriomeningitis virus.[4] Further development of multiple virus detection systems is required to increase coverage of a range of virus strains and subtypes. We have experienced pandemics, such as WNV in the United States in 2003 and the chikungunya virus on Reunion Island in 2006; thus, there is a need to develop a rapid virus detection system that uses a more flexible blood-testing platform and meets the safety requirements for transfusion.

HBV is one of the most geographically widespread viruses and is subdivided into eight main genotypes (A–H),[5,6] causing liver cirrhosis and hepatocellular carcinoma. Although most infectious blood units are removed by screening for hepatitis B surface antigen (HBsAg), there is clear evidence that transmission by HBsAg-negative components occurs during the serologically negative window period and late stages of infection.[7] In addition to the window period of infection, HBV blood screening is required to detect all virus genotypes. Similar to HBV, several false-negative results in minipool NAT screening were reported after the introduction of WNV NAT because of the low viral load. Moreover, WNV continues to diverge rapidly from the originally isolated strain.[8,9] Multiplex NAT assays have become the modern method for detecting several viruses, and in conjunction with automated systems, they have the potential to improve processes that ensure blood safety. Candotti and colleagues[10] have reported the feasibility of a multiplex real-time quantitative reverse-transcriptase polymerase chain reaction (PCR) for HBV, HCV, and HIV-1, suggesting that simultaneous amplification of multiple pathogens is an effective approach for improving pathogen detection methods. The flexibility provided by multiplex PCR is limited, however, because the PCR primers are designed in commonly preserved regions of the viral genomes. To increase the detectable range for multiple pathogens, PCR using degenerate primers has been developed. Recently, bioinformatics has strongly improved the design of degenerate primers, allowing the coverage of a wide range of virus subtypes. We have developed a new method for designing degenerate primers.[11] Here, we used the diamond-like carbon-coating microarray chip (DLC-chip) to reduce background noise and increase the detection sensitivity of the system.[12,13] We combined two newly developed technology platforms for a multiple pathogen detection system using a degenerate PCR–based NAT system (dPCR-NAT).

MATERIALS AND METHODS

Design of dPCR primers and microarray oligoprobes

We designed dPCR primers that hybridized with HIV, HCV, HBV, human parvovirus B19 (PVB19), and WNV genomic sequences (Table 1). We used the CoCoMo (Coordination of Common Motifs) algorithm (www.geneknot.info/cocomo)[14] for dPCR primer design. CoCoMo determines primer regions in commonly conserved nucleotide regions in the assembled nucleotide sequences of virus strains. In each case, all viral sequences were identified from GenBank and EMBL, and a low degeneracy primer set was selected as a candidate using the CoCoMo algorithm. We collected data on 2072 HIV-1 nucleotide sequences and selected 14 complete genome sequences that corresponded to each genotype of HIV-1. We designed dPCR primer sets for detecting 14 complete genome sequences, resulting in approximately 3897

Virus	Probe name	Sequence (5'-3')	Tm (°C)*
HIV	IR1-1	ACTATTCTTTCCCCTGCACTGTACCCCCCAATCC	78
	IR1-2	TCTGTTGCTATTATGTCTACTATTCTTTCCCC	66
	IR1-3	CTTTAGTTTGTATGTCTGTTGCTATTATGTCTAC	63
	IR1-4	GTAATTTGTTTTTGTAATTCTTTAGTTTGTATGTCTG	66
	IR3-1	GGGATTGTAGGGAATTCCAAATTCCTGCTTGATT	76
	IR3-3	CTTTAATTCTTTATTCATAGATTCTACTACTCCTTGACTTTG	69
HCV	CF1-1	AACCGGTGAGTACACCGGAATTGCCAGGAC	77
	CF1-2	TTTCTTGGATCAACCCGCTCAATGCCTGGAGATTTGGGCG	88
	CF1-3	TGCCCCCGCAAGACTGCTAGCCGAGTAGTGTTGGG	85
	CF2-1	AGAGCCATAGTGGTCTGCGGAACCGGTGAGTACACCGGA	86
	CF2-2	CTAGCCGAGTAGTGTTGGGTCGCGAAAGGCCTTG	81
	CF2-3	GCGAAAGGCCTTGTGGTACTGCCTGATAGGGTGCT	82
	CR2-1	TCCGGTGTACTCACCGGTTCCGCAGACCACTATGGCTCT	86
HBV	BF4-1	CTGCTATGCCTCATCTTCTTGTTGGTTCTTCTGG	75
	BF4-2	CTTCTGGATTATCAAGGTATGTTGCCCGTTTGTCCTC	78
	BF4-3	TGTCCTCTAATTCCAGGATCAACAACAACCAGTAC	73
	BF4-4	ATTCCCATCCCATCGTCCTGGGCTTTCGCAAAATACC	84
	BF4-5	CCTATGGGAGTGGGCCTCAGTCCGTTTCTCTTGGCTC	84
	BF4-6	GTCCGTTTCTCTTGGCTCAGTTTACTAGTGCCATTTGTTCAG	80
	BR4-1	CCAGAAGAACCAACAAGAAGATGAGGCATAGCAG	75
PVB19	PVB19F-1	GGCGCCTGGAACACTGAGACCCCGCGCTCTAGTAC	85
	PVB19F-2	GGCGCCTGGAACACTGAAACCCCGCGCTCTAGTAC	84
	PVB19F-3	GAACTCAGTGAAAGCAGCTTTTTCAACCTCATCACTCC	78
	PVB19R-1	GTACTAGAGCGCGGGGTCTCAGTGTTCCAGGCGCC	85
	PVB19R-2	GTACTAGAGCGCGGGGTTTCAGTGTTCCAGGCGCC	84
	PVB19R-3	GGAGTGATGAGGTTGAAAAAGCTGCTTTCACTGAGTTC	78
WNV	WNVF-1	ATGATTGATCCTTTTCAGCTGGGCCTTCTGGT	77
	WNVF-2	ATGATTGACCCTTTTCAGTTGGGCCTTCTGGTCG	80
	WNVF-3	ATGATTGATCCTTTTCAGCTGGGCCTTCTGGT	77
	WNVF-4	ACGCCGACATGATTGATCCTTTTCAGTTGGGCCT	81
	WNVR-1	ACCAGAAGGCCCAGCTGAAAAGGATCAATCAT	77
	WNVR-2	CGACCAGAAGGCCCAACTGAAAAGGGTCAATCAT	80
	WNVR-3	ACCAGAAGGCCCAGCTGAAAAGGATCAATCAT	77
	WNVR-4	AGGCCCAACTGAAAAGGATCAATCATGTCGGCGT	81
IC	IC-1	GTCGTAGTTCCGACCATAAACGATGCCGACCGG	81
	IC-2	GGCGATGCGGCGGCGTTATTCCCATGACCC	86
	IC-3	CCGCCGGGCAGCTTCCGGGAAACCAAAGTCTTTG	87
	IC-4	TCGAAGACGATCAGATACCGTCGTAGTTCCGACC	78
QC	QC	TTGGCAGAAGCTATGAAACGATATGGG	69

TABLE 2. Oligonucleotide probe sequences of DNA microarray assay

* The melting temperature (Tm) was calculated using NetPrimer (PREMIER Biosoft International, http://www.premierbiosoft.com/).

primer sets. For HCV, we collected 978 sequences and selected 167 complete genome sequences to design dPCR primer sets, generating 31 primer sets. For HBV, 1461 sequences were collected and 1344 complete genome sequences were selected to generate the dPCR primer sets, generating approximately 29 primer sets. For WNV, we collected 17,172 sequences and used 111 complete genome sequences to design the dPCR primer sets, generating 1649 primer sets. For PVB19, we collected 1145 sequences and selected seven complete genome sequences to design the dPCR primer sets, generating 2517 primer sets. Selected primers are listed in Table 1. The sequences of the oligonucleotide detection probes on the DLC-chip are indicated in Table 2. The probes were manually designed from regions amplified by the degenerate primers. Thirty to 42 oligomers that had a GC content between 50 and 60% were selected. The resultant melting temperature values were 62 to 88°C. The hybridization stability of the PCR fragments was biased according to strand; therefore, we designed probes on each strand of the PCR products (sense strand—same sense as forward primer).

Synthesis of genotype panel oligomers for screening primers

Genotype panel oligomers of HIV-1, HBV, PVB19, and WNV were prepared by overlap-extension PCR (OE-PCR;[15] Fig. 1A). Regions for OE-PCR were selected according to the nucleotide sequences amplified with our primers for each virus genotype. The nucleotide sequences of HBV subtypes B and C panel oligomers had the same sequence. The joining oligonucleotides listed in Supplemental Table S1 (available as supporting information in the online version of this paper) were designed using DNA works (http://helixweb.nih.gov/dnaworks/).[16] The nucleotide sequences of each genotype panel oligomers are listed in Supplemental Table S2 (available as supporting information in the online version of this paper). OE-PCR
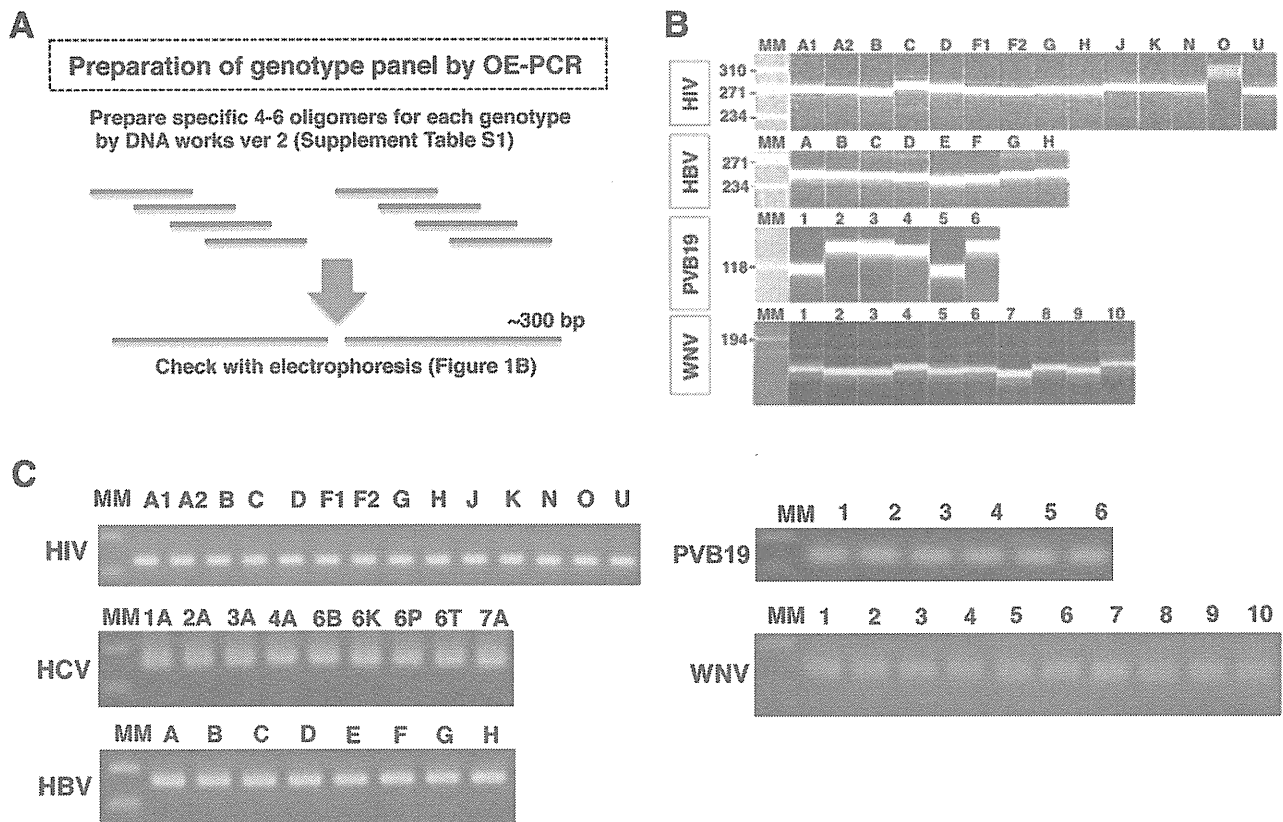
Fig. 1. Synthesis of genotype panel oligomers for HIV, HCV, HBV, PVB19, and WNV. (A) Preparation of genotype panel oligomers by PCR-based gene synthesis, OE-PCR. dPCR primers were validated with genotype panel oligomers. (B) Genotype panel oligomers were synthesized against 14 subtypes of HIV-1, eight genotypes of HBV, nine genotypes of HCV, six genotypes of PVB19, and 10 genotypes of WNV. (C) Each of the HIV-1 subtype oligomers was amplified by dPCR primers for HIV-1. The top panel shows the agarose gel electrophoresis analysis of PCR products to identify the 14 HIV-1 subtypes. Similar results were obtained from HCV, HBV, PVB19, and WNV genotype panel oligomers with specific dPCR.

was carried out according to a two-step reaction method by using a PCR kit (Prime Star, Takara-bio, Otsu, Japan; Fig. 1). The first reaction was carried out using a mixture of OE-PCR oligomers in 30 cycles of 98°C for 15 seconds, 55°C for 10 seconds, and 72°C for 15 seconds. One microliter of the first PCR products was transferred to the second PCR solution, which included 5 pmol/μL each of the 5′- and 3′-end primers. The second reaction consisted of 30 cycles at the temperature conditions used in the first reaction. The molecular weights of the OE-PCR products were checked on a chip electrophoresis system (Multina 202, Shimazu, Kyoto, Japan; Fig. 1B). HCV genotype panel oligomers were synthesized and obtained from Invitrogen (Carlsbad, CA; custom DNA oligonucleotide synthesis service).

Viral samples for dPCR-based NAT

For more accurate analysis, we purchased PVB19 NAT-based assays genotype panel (First International Standard; Category Number, 09/110 National Institute for Biological Standards and Control [NIBSC], UK); HIV-1 RNA genotype panel (Category Number 08/358 NIBSC); HCV RNA genotype panel (Category Number 08/264 NIBSC); HCV for NAT (Fourth WHO International Standard; Category Number 06/102 NIBSC); HBV for NAT (Third WHO International Standard; Category Number 10/264 NIBSC); and PVB19 DNA NAT assays (Second International Standard; Category Number 99/802 NIBSC). To evaluate the specificity of our dPCR-NAT system, we diluted each genotype panel with defibrinated plasma (Basematrix 53, SeraCare BBI Diagnostics, Milford, MA) to give a final concentration of 151 to 9722 copies/mL (HIV), 500 to 1500 IU/mL (HCV), 5754 to 123,027 IU/mL (HBV), and 870,964 to 954,933 IU/mL (PVB19), respectively. To evaluate the sensitivity of our dPCR-NAT system, we diluted each international standard with defibrinated plasma to give a final concentration of 1 to 10,000 IU/mL. Samples containing the New York strain of WNV RNA (NY 2001-6263; NATtrol, Category Number NATWNV-0005,

1 mL, 50,000 copies/mL) were purchased from Zepto-Metrix (Buffalo, NY) and were diluted with defibrinated plasma to give a final concentration of 1 to 1000 copies/mL. Blood specimens from healthy volunteer donors who were confirmed as negative for HCV, HBV, and HIV were provided from Japan Red Cross and used as a negative control.

DNA and RNA extraction, reverse transcription, and PCR amplification

Each viral DNA and RNA was extracted from 200 µL of diluted sample with a viral nucleic acid kit and a viral RNA kit (High Pure, Roche, Basel, Switzerland). Total RNA of HCV, HIV-1, and WNV were all reverse transcribed with a cDNA synthesis kit (Superscript III RT, Invitrogen) according to the manufacturer's protocol. Twenty-microliter cDNA samples were prepared for PCR amplification of each virus. The PCR was carried out with PCR mixture (GoTaq, Promega, Madison, WI). In the PCR mixture, diluted nucleic acid and 50 µmol/L of each degenerate primer were included. The reaction consisted of 50 cycles of 94°C for 30 seconds, 55°C for 30 seconds, and 72°C for 60 seconds. We used 5 ng of human cDNA fragment as an internal control (IC).

Microchip fabrication

We purchased 3-mm² silicon DLC-chip from Toyo Kohan (Tokyo, Japan). Each probe was spotted by Spotarray 72 (Perkin-Elmer, Waltham, MA) with a 250-µm spot distance and 100-µm-diameter spots. Spotted probes were baked for 60 minutes at 80°C. We made DNA chips to evaluate probe sensitivity and for detection of viral samples, including WHO International Standards and WHO genotype panels. Each sequence for detection probes on the chip is listed in Table 2.

Synthesis and hybridization of fluorescently labeled DNA samples

PCR amplification of extracted DNA or cDNAs was performed for fluorescent labeling using polymerase (GoTaq, Promega) with Cy-5 dCTP. The PCR mixture included template DNA or cDNA, 50 µmol/L primers, 0.5 µL of Cy-5 dCTP (Perkin-Elmer), 1 µL of dNTP mixture (2.5 mmol/L each, 0.25 mmol/L dCTP), 5 µL of 5× PCR buffer (GoTaq, Promega), and 0.25 µL of polymerase (GoTaq, Promega). The 50-cycle PCR profile was 94°C for 30 seconds, 55°C for 30 seconds, and 72°C for 30 seconds. Amplification was carried out in a PCR system (GeneAmp 9700, Applied Biosystems, Foster City, CA). Two microliters of the PCR-amplified reaction mixture was hybridized with the chip for 30 minutes at 50°C. The hybridized chip was washed with saline-sodium citrate buffer and scanned with a fluo-rescent scanner (FLA-8000, Fujifilm, Tokyo, Japan). Geographic origin was estimated from the obtained fluorescence patterns, thereby indicating specific genotypes.

Transcription-mediated amplification assay

To validate our assay sample preparation including viral DNA or RNA, we performed transcription-mediated amplification (TMA) assays for HBV, HCV, and HIV-1 by using an assay kit (Ultrio, Novartis Pharma, Tokyo, Japan) according to the manufacturer's protocol.

RESULTS

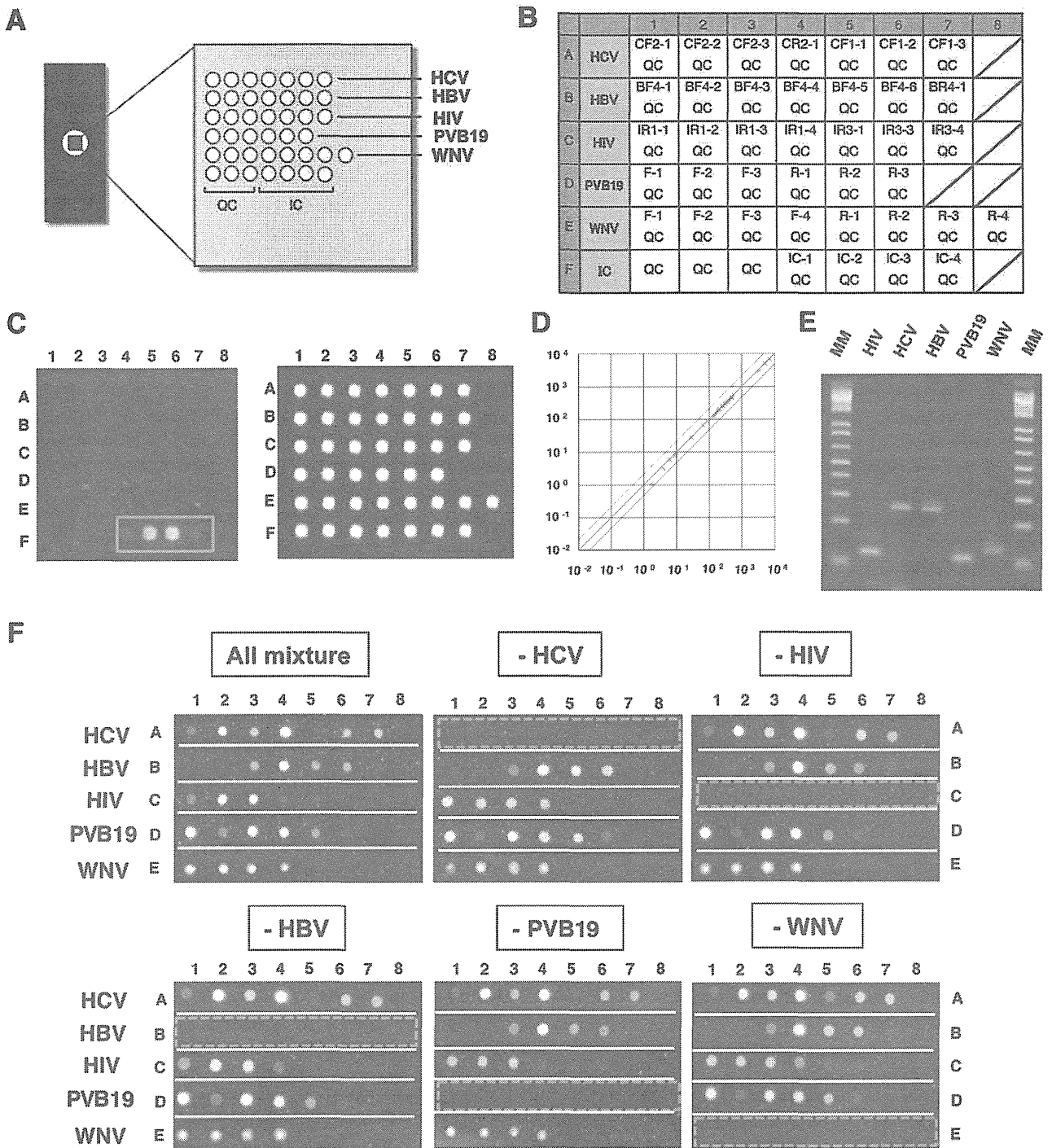## Synthesis of genotype panel oligomers by OE-PCR

To verify our designed dPCR primers, we prepared genotype panel oligomers (100-300 bp) as viral genotype reference materials for HIV (A1, A2, B, C, D, F1, F2, G, H, J, K, N, O, and U), HBV (A–H), WNV (1-10), and PVB19 (1-6) made by OE-PCR (Fig. 1A). The target regions for OE-PCR were selected according to the nucleotide sequences of the standard strain for dPCR and the DLC-chip detection system (Supplemental Table S2). The joining oligonucleotides were designed using an online computer program (DNAWorks, Version 2, http://helixweb.nih.gov/dnaworks/). The nucleotide sequences of each genotype panel oligomer are listed in Supplemental Table S1. OE-PCR was carried out according to a two-step reaction method. The OE-PCR products were checked on a chip electrophoresis system (Multina 202, Shimazu). As expected, we could detect our OE-PCR products at appropriate molecular size (Fig. 1B). For HCV (1A, 2A, 3A, 4A, 6B, 6K, 6P, 6T, and 7A), genotype panel oligomers were designed and made by custom service (Invitrogen).

Validation of dPCR primer for detection of virus genotype panel oligomers

We confirmed whether our designed primers could specifically amplify each virus subtype by PCR. The PCR products for all HIV, HCV, HBV, PVB19, and WNV subtypes were detected at the expected size by gel electrophoresis (Fig. 1C).

QC of our pathogen detection DNA microarray system

To evaluate specificity of each probe in our DLC-chip, the detection ability of our probes was analyzed. We selected 36 specific probe sets that had high detection abilities (>50% of genotypes) from the 53 originally designed evaluated probes (data not shown) and then spotted them on DLP-Chip (Fig. 2A, B). DNA microarray images were

A

B

		1	2	3	4	5	6	7	8
A	HCV	CF2-1 QC	CF2-2 QC	CF2-3 QC	CR2-1 QC	CF1-1 QC	CF1-2 QC	CF1-3 QC	
B	HBV	BF4-1 QC	BF4-2 QC	BF4-3 QC	BF4-4 QC	BF4-5 QC	BF4-6 QC	BR4-1 QC	
C	HIV	IR1-1 QC	IR1-2 QC	IR1-3 QC	IR1-4 QC	IR3-1 QC	IR3-3 QC	IR3-4 QC	
D	PVB19	F-1 QC	F-2 QC	F-3 QC	R-1 QC	R-2 QC	R-3 QC		
E	WNV	F-1 QC	F-2 QC	F-3 QC	F-4 QC	R-1 QC	R-2 QC	R-3 QC	R-4 QC
F	IC	QC	QC	QC	IC-1 QC	IC-2 QC	IC-3 QC	IC-4 QC	

C

D

E

F

captured by an image analyzer (FLA-8000, Fuji Photo Film, Tokyo, Japan). Hybridized slides were inserted in the FLA-800, and the scan conditions were set as 10 µm resolution, standard scan mode, and photomultiplier tube high-value 100% laser. Saved DNA microarray images were analyzed, and fluorescent intensity of each spot was measured using a computer program (ArrayGauge Software, Fuji Photo Film). After removing the background

signal, we defined the positive signal standard as radio intensity more than five times higher than background. The signal intensity was calculated as the total pixel value minus the global background. The signal intensities were then normalized to the mean for all the spots in the array.

To determine the specificity of the new system, we applied two different QCs: an IC probe (oligonucleotide complementary to the Cy5-labeled amplicon of the 18S

Fig. 2. (A) Schematic design of DLC-chip, including HIV, HCV, HBV, WNV, and PVB19 probes (B) and their relative position in the slide layout. Spotted probes of seven subtypes of HIV-1, seven genotypes of HCV, seven genotypes of HBV, six genotypes of PVB19, and eight genotypes of WNV were selected. All of the probes were spotted together on the chip, along with the QC probes. (C) Evaluation of the detection system using the IC (left panel) and QC (right panel). Anti-IC probes specifically hybridized to and amplified 18S rRNA PCR product from human DNA. (D) QC by using same amplified sample. Correlation coefficients using scatter plot indicated that each DLC-chip was highly reproducible, with a correlation of 0.99905. (E) Multiple detection system for five virus genomes. Agarose gel electrophoresis analysis of PCR products to detect HIV-1, HCV, HBV, PVB19, and WNV. These PCR products were positive on the microarrays. (F) Multiple detection system for five viruses by DLC-chip. The PCR products of five viruses were mixed at the following concentrations: HCV, 10 IU/mL; HBV, 10 IU/mL; HIV-1, 10,000 IU/mL; PVB19, 10 IU/mL; and WNV, 10 copies/mL. Each panel used a mixture of the five viruses that lacked HIV-1, HCV, HBV, PVB19, or WNV. The red line indicates the row where excluded virus was not detected. Cross-hybridization between the five viruses was not confirmed.

rRNA gene; Fig. 2C, left) and a QC probe (oligonucleotide complementary to the Cy3-labeled QC probe; Fig. 2C right). This allowed us not only to monitor the spot uniformity, but also to detect potential irregularities during the hybridization process. To evaluate the reproducibility of our DLC-chip, we hybridized the same PCR-amplified samples to different DLC-chips and measured each signal intensity. Correlation coefficients using scatter plots indicated that each DLC-chip was highly reproducible, showing a correlation of 0.99905 (Fig. 2D).

Multiple detection of five viruses in one test

We determined whether our designed probes could detect the PCR products of all the HIV genotypes. On the DLC-chip, seven different HIV-1–specific probes were aligned. After being labeled with Cy5, PCR products were detected by hybridization to HIV-specific probes on the DLC-chip. We considered that a sample was positive if at least two different probes showed a positive signal. These HIV-1–specific degenerative primer and probe sets detected all of the following genotypes: A1, A2, B, C, D, F1, F2, G, H, J, K, N, O, and U (data not shown). Similar to the HIV detection system, different probe sets detected all the HCV, HBV, PVB19, and WNV genotypes (data not shown). To determine the ability to detect multiple viruses on one DNA chip, we separately performed virus-specific genome amplification (Fig. 2E) and mixed each PCR product in one tube and hybridized the PCR products onto the DLC-chip. The mixed viral PCR product (HIV, HCV, HBV, PVB19, and WNV) was readily detected as a hybridized spot on the DCL-chip (Fig. 2F). We prepared a mixed sample minus one virus amplicon as a negative control for cross-hybridization and nonspecific binding. We confirmed that no cross-hybridization occurred with HIV-1, HCV, HBV, PVB19, and WNV.

Specificity and sensitivity of our dPCR-NAT system by using WHO genotype panels and international standards

To determine the specificity of our DNA microarray system to detect each virus genotype, we prepared the

WHO genotype panel samples for each virus. For WNV, we used the genotype panel oligomer described in Figure 1 as an NAT genotype panel because there was no commercially available panel. We extracted DNA or RNA from each genotype panel for HIV, HCV, HBV, PVB19, and WNV. Each template DNA or cDNA was amplified with each dPCR primer listed in Table 1. The amplified PCR products for all genotypes of each virus were confirmed on 3% agarose gels and DNA chips. We detected all the HIV, HCV, HBV, PVB19, and WNV genotypes (Fig. 3B). Our DNA microarray data are summarized in Supplemental Table S4 (available as supporting information in the online version of this paper). To validate the sensitivity of our NAT system, we used WHO International Standards as reference materials. To check our reference samples, we performed FDA-licensed NAT assays using a TMA assay (Supplemental Table S3, available as supporting information in the online version of this paper) before analysis. For sensitivity assay, we prepared HCV RNA, HBV, and PVB19 from NIBSC. These materials were used as international standards for NAT quality assurance. We prepared each sample to give a final concentration of 1 to 10,000 IU/mL and isolated DNA or RNA from 200-μL samples. Thus, each sample was assumed to contain 0.2 to 2000 IU virus if extraction efficiency was 100%. DNA and RNA were extracted. RNA samples were all reverse transcribed with a cDNA synthesis kit (Superscript III RT, Invitrogen), and all cDNA samples were used for PCR. We detected 1 IU/mL HCV, 1 IU/mL HBV, 1 IU/mL PVB19, and 1 copy/mL WNV (Fig. 3C). Similar results were obtained from at least three independent experiments. For HIV, we estimated the detection limit in at least five independent tests. We detected 10,000 IU/mL for 100%, 1000 IU/mL for 77%, 100 IU/mL for 7%, 10 IU/mL for 0%, and 1 IU/mL sample for 0%. Thus we conclude that our system could detect 1000 IU/mL equivalent to 200 IU/PCR sample for HIV. Detection limits for each virus are listed in Table 3.

DISCUSSION

We investigated the performance of the new NAT system using dPCR primers and a DLC-chip. We showed that our NAT system was specific for HIV-1, HCV, HBV, PVB19, and

A

Preparation samples → 1-10,000 IU/mL sample

- WHO genotype panel
- WHO International Standard
- WNV: NATrol and OE-PCR
- Prepare 1 to 10,000 IU/mL samples

Extraction of DNA/RNA

200uL sample → DNA RNA Extraction

1 IU/mL = 0.2 IU/sample
10 IU/mL = 2 IU/sample
100 IU/mL = 20 IU/sample
1,000 IU/mL = 200 IU/sample
10,000 IU/mL = 2,000 IU/sample

HIV/HCV/WNV RNA→RT
HBV/PvB19 DNA

PCR Amplification

PCR reaction

Detection with DNA Chip

Check with DNA microarray

B

WHO Genotype Panel

OE-PCR

C

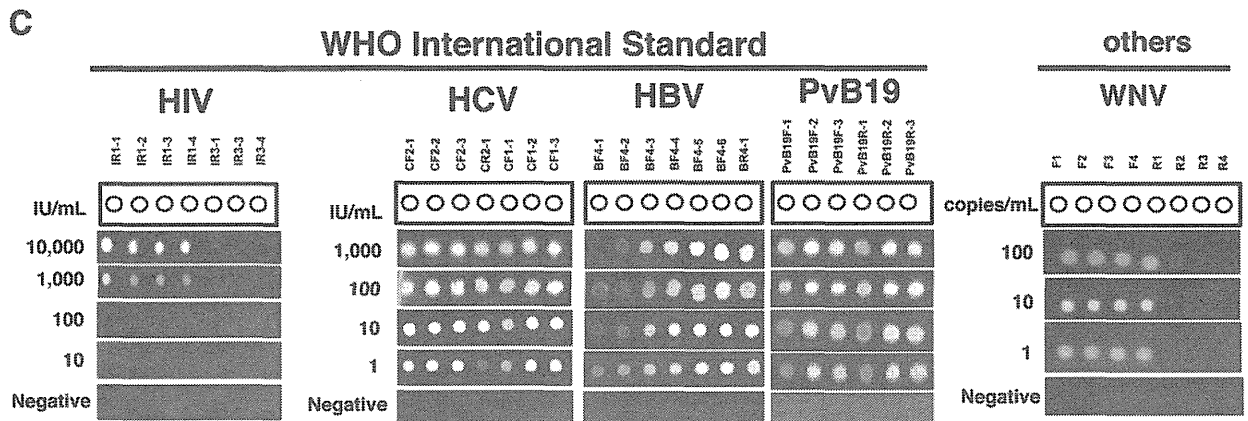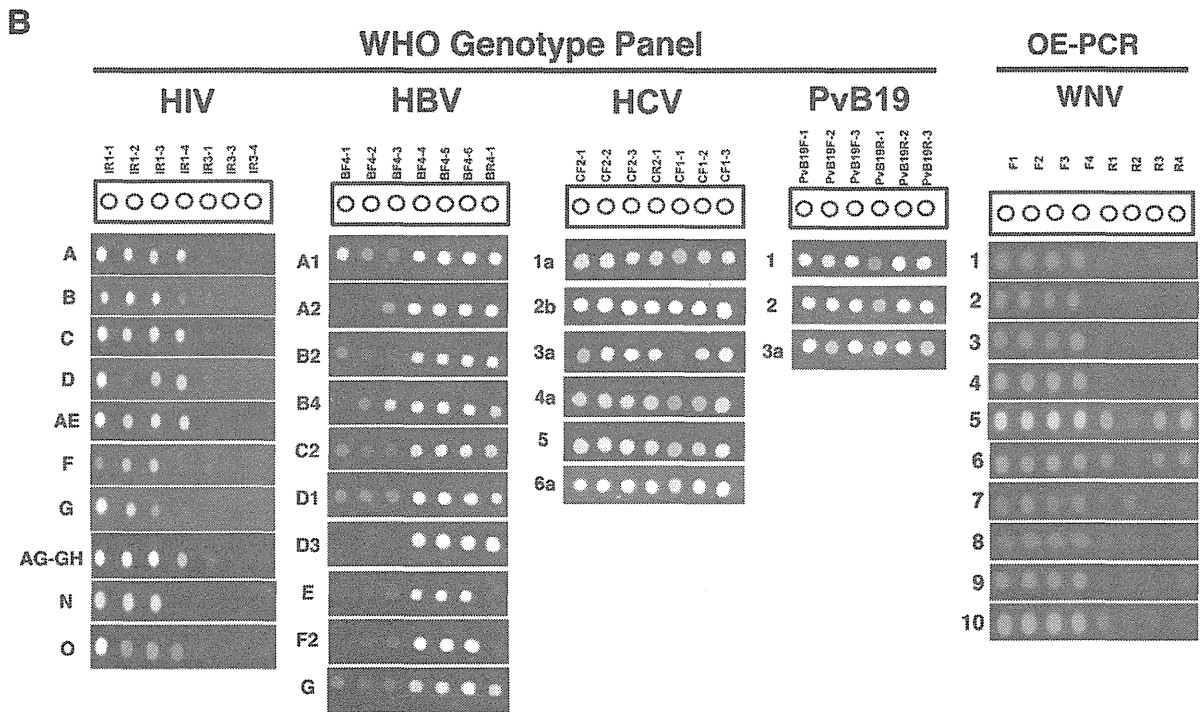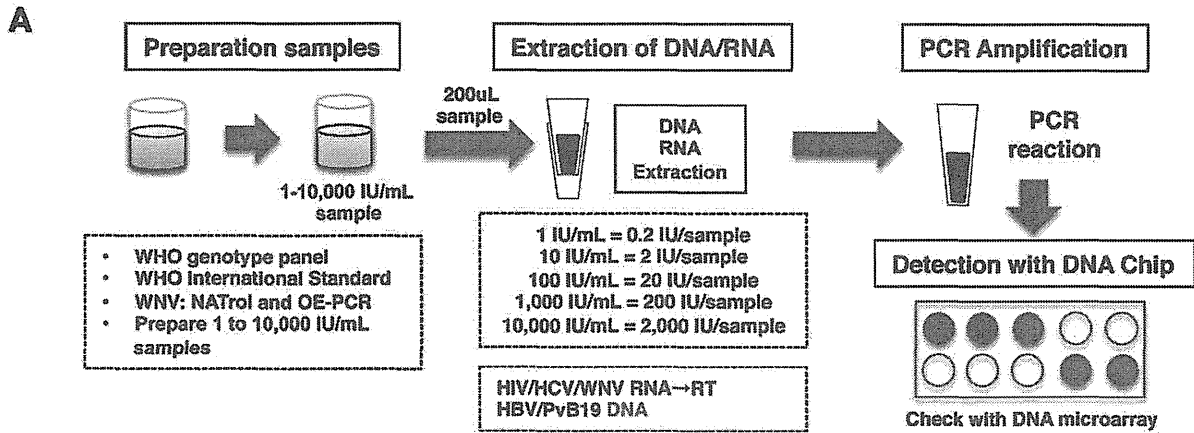### WHO International Standard

others

Fig. 3. (A) Schematic illustration of sensitivity analysis of our detection system, including extraction process. Detection of the isolated virus genomes from human plasma sample. Samples containing HIV-1, HCV, and HBV were diluted with defibrinated plasma (Basematrix 53; SeraCare) at 1 to 10,000 IU/mL. (B) For more accurate analysis, we prepared a WHO genotype panel for HIV-1, HBV, HCV, and PVB19. We detected all genotypes by using our designed degenerated primer. (C) For sensitivity analysis of our NAT system, we prepared WHO International Standards for HIV-1, HCV, HBV, and PVB19. We diluted these materials with negative sera at 1 to 10,000 IU/mL and extracted DNA and RNA from 200-μL samples. All RNA samples were transcribed with Superscript III. We detected HIV at 1000 IU/mL, HCV at 1 IU/mL, HBV at 1 IU/mL, and PVB19 at 1 IU/mL.

◄───

TABLE 3. Detection limit of our dPCR-NAT system*				
IU/mL	HIV (%)	HCV (%)	HBV (%)	PVB19 (%)
10,000	100	100	100	100
1,000	77	100	100	100
100	7	100	100	100
10	0	100	100	100
1	0	50	25	75

* % positive: Reactive/Tested (Percent Reactive). The measurement obtained in each specimen was tested with two sample lots in two independent test assays. For HIV, we tested five sample lots in five independent test assays.

WNV at low viral loads. In addition, we showed that our system detected various virus genotypes. Degenerate primers are useful not only for detecting unknown genes, but also for the simultaneous amplification of mutated genes.[17] In the case of viruses, many mutated strains appear in a particular geographical area and at a specific time.[18] Recently, we used CoCoMo primers, a fully automatic design pipeline for PCR primers, according to the CodeHop primer design strategy, by which others can analyze the oligonucleotide motif incidence.[14] The CoCoMo program is available online (www.geneknot. info/cocomo). We utilized CoCoMo primers to design the primer sequences in this study. The algorithm-designed primers were confirmed to fit most subtypes or genotypes of the target viruses (Table 1) and enabled efficient detection of a wide range of viruses. In general, PCR procedures with the degenerate primers had lower sensitivity than that of the specific primers. To overcome this disadvantage, we used fluorescence detection on the DLC-chip, which provided higher sensitivity.[12] Additionally, the degenerate primer set was designed to detect the polymorphic region of the viral genome; therefore, subtypes or genotypes could be discriminated on the DLC-chip. The combination of the primers and DLC-chips was therefore validated. These results suggest that the combination of dPCR and DLC-chips is beneficial for blood-borne virus detection. To increase the safe use of the system, automation of our detection system will be required in the future.

A low level of HBV may proliferate in transfused recipients who are immunocompromised or immunosuppressed. In addition, the window period of HBV is relatively long, but the presence of HBV DNA without detectable HBsAg outside the window period, known as occult HBV infection, has been reported.[7] This suggests that the development of a highly sensitive detection system for HBV is particularly important. Although the current TMA sensitivity corresponds to 1 to 5 IU/mL at the reproductive level, using the same viral samples in this study we detected 1 to 10 IU/mL HBV. These data suggest that the sensitivity of our analysis system is equivalent to that of the TMA assay (Fig. 3C). Thus far, HBV Genotype C is the most prevalent genotype in Japan (85%), while the prevalence of Genotypes A and D is 1.7 and 0.4%, respectively.[19-21] Currently, the level of Genotype A is increasing in the younger generation because of horizontal infection.[11,22,23]

For HIV-1 detection and quantification, various methods have been developed, but most real-time techniques involve their sensitivity to point mutations within primer and probe target sequences. Our dPCR-NAT system could detect a wide range of HIV genotypes by using dPCR primers. Despite the wide range of genotype detection, sensitivity was not high. We could detect 200 IU HIV/PCR procedure. Improvement is needed for HIV dPCR sensitivity. Similarly for HBV and HCV, the next-generation virus detection system must be able to cope with this situation, namely, by possessing a wide detectable viral genotype range and a low detection level. With our detection system, all of the virus genotypes were detected at 1 to 1000 IU/mL sample. Previous studies by Hsia and coworkers[24] combined multiplex PCR and DNA chips and detected three different viruses in a single sample. Our mixed PCR product data (Fig. 2F) indicated that our system could simultaneously detect five different viruses in one DNA chip. These data suggest that our system is suitable for multiple pathogen testing.

In conclusion, the dPCR-NAT system is an accurate and reliable test for HIV, HBV, HCV, PVB19, and WNV detection with respect to specificity, sensitivity, and genotype inclusivity and a reproducible assay for the detection of multiple blood-contaminating pathogens.

CONFLICT OF INTEREST

All authors concur with submission of this manuscript, and we affirm that the material submitted has not previously been reported, and is not under consideration for publication elsewhere. We do not have any conflicting financial interests.

REFERENCES

1. Tabor E, Epstein JS. NAT screening of blood and plasma donations: evolution of technology and regulatory policy. Transfusion 2002;42:1230-7.
2. Stramer SL, Hollinger FB, Katz LM, Kleinman S, Metzel PS, Gregory KR, Dodd RY. Emerging infectious disease agents and their potential threat to transfusion safety. Transfusion 2009;49(Suppl 2):1S-29S.
3. Lelie PN, Cuypers HTM, van Drimmelen AAJ, Quint WGV. Quality assessment of hepatitis C virus nucleic acid amplification methods. Infus Ther Transfus Med 1998;25:102-10.
4. Fischer SA. Emerging viruses in transplantation: there is more to infection after transplant than CMV and EBV. Transplantation 2008;86:1327-39.
5. Kramvis A, Kew M, François G. Hepatitis B virus genotypes. Vaccine 2005;23:2409-23.
6. Norder H, Couroucé AM, Coursaget P, Echevarria JM, Lee SD, Mushahwar IK, Robertson BH, Locarnini S, Magnius LO. Genetic diversity of hepatitis B virus strains derived worldwide: genotypes, subgenotypes, and HBsAg subtypes. Intervirology 2004;47:289-309.
7. Allain JP. Occult hepatitis B virus infection: implications in transfusion. Vox Sang 2004;86:83-91.
8. Pealer LN, Marfin AA, Petersen LR, Lanciotti RS, Page PL, Stramer SL, Stobierski MG, Signs K, Newman B, Kapoor H, Goodman JL, Chamberland ME. West Nile Virus Transmission Investigation Team. Transmission of West Nile virus through blood transfusion in the United States in 2002. N Engl J Med 2003;349:1236-45.
9. Grinev A, Daniel S, Stramer S, Rossmann S, Caglioti S, Rios M. Genetic variability of West Nile virus in US blood donors, 2002-2005. Emerg Infect Dis 2008;14:436-44.
10. Candotti D, Temple J, Owusu-Ofori S, Allain JP. Multiplex real-time quantitative RT-PCR assay for hepatitis B virus, hepatitis C virus, and human immunodeficiency virus type 1. J Virol Methods 2004;118:39-47.
11. Kobayashi M, Ikeda K, Arase Y, Suzuki F, Akuta N, Hosaka T, Sezaki H, Yatsuji H, Kobayashi M, Suzuki Y, Watahiki S, Mineta R, Iwasaki S, Miyakawa Y, Kumada H. Change of hepatitis B virus genotypes in acute and chronic infections in Japan. J Med Virol 2008;80:1880-4.
12. Gao Y, Chen X, Gupta S, Gillis KD, Gangopadhyay S. Magnetron sputtered diamond-like carbon microelectrodes for on-chip measurement of quantal catecholamine release from cells. Biomed Microdevices 2008;10:623-9.
13. Iwafune Y, Tan JZ, Ino Y, Okayama A, Ishigaki Y, Saito K, Suzuki N, Arima M, Oba M, Kamei S, Tanga M, Okada T, Hirano H. On-chip identification and interaction analysis

of gel-resolved proteins using a diamond-like carbon-coated plate. J Proteome Res 2007;6:2315-22.
14. Jimba M, Takeshima SN, Matoba K, Endoh D, Aida Y. BLV-CoCoMo-qPCR: quantitation of bovine leukemia virus proviral load using the CoCoMo algorithm. Retrovirology 2010;7:91.
15. Hoover DM, Lubkowski J. DNAWorks: an automated method for designing oligonucleotides for PCR-based gene synthesis. Nucleic Acids Res 2002;30:e43.
16. Dong B, Mao R, Li B, Liu Q, Xu P, Li G. An improved method of gene synthesis based on DNA works software and overlap extension PCR. Mol. Biotechnol 2007;37:195-200.
17. Moonka D, Loh EY. A consensus primer to amplify both alpha and beta chains of the human T cell receptor. J Immunol Methods 1994;169:41-51.
18. Ha C, Coombs S, Revill PA, Harding RM, Vu M, Dale JL. Design and application of two novel degenerate primer pairs for the detection and complete genomic characterization of potyviruses. Arch Virol 2008;153:25-36.
19. Orito E, Ichida T, Sakugawa H, Sata M, Horiike N, Hino K, Okita K, Okanoue T, Iino S, Tanaka E, Suzuki K, Watanabe H, Hige S, Mizokami M. Geographic distribution of hepatitis B virus (HBV) genotype in patients with chronic HBV infection in Japan. Hepatology 2001;34:590-4.
20. Sugauchi F, Kumada H, Sakugawa H, Komatsu M, Niitsuma H, Watanabe H, Akahane Y, Tokita H, Kato T, Tanaka Y, Orito E, Ueda R, Miyakawa Y, Mizokami M. Two subtypes of genotype B (Ba and Bj) of hepatitis B virus in Japan. Clin Infect Dis 2004;38:1222-8.
21. Sugauchi F, Kumada H, Acharya SA, Shrestha SM, Gamutan MT, Khan M, Gish RG, Tanaka Y, Kato T, Orito E, Ueda R, Miyakawa Y, Mizokami M. Epidemiological and sequence differences between two subtypes (Ae and Aa) of hepatitis B virus genotype A. J Gen Virol 2004;85:811-20.
22. Yoshikawa A, Gotanda Y, Suzuki Y, Tanaka M, Matsukura H, Shiraishi T, Matsubayashi K, Kon E, Suzuki K, Yugi H; Japanese Red Cross HBV Genotype Research Group. Age- and gender-specific distributions of hepatitis B virus (HBV) genotypes in Japanese HBV-positive blood donors. Transfusion 2009;49:1314-20.
23. Matsuura K, Tanaka Y, Hige S, Yamada G, Murawaki Y, Komatsu M, Kuramitsu T, Kawata S, Tanaka E, Izumi N, Okuse C, Kakumu S, Okanoue T, Hino K, Hiasa Y, Sata M, Maeshiro T, Sugauchi F, Nojiri S, Joh T, Miyakawa Y, Mizokami M. Distribution of hepatitis B virus genotypes among patients with chronic infection in Japan shifting toward an increase of genotype A. J Clin Microbiol 2009;47:1476-83.
24. Hsia CC, Chizhikov VE, Yang AX, Selvapandiyan A, Hewlett I, Duncan R, Puri RK, Nakhasi HL, Kaplan GG. Microarray multiplex assay for the simultaneous detection and discrimination of hepatitis B, hepatitis C, and human immunodeficiency type-1 viruses in human blood samples. Biochem Biophys Res Commun 2007;356:1017-23.

SUPPORTING INFORMATION

Additional Supporting Information may be found in the online version of this article at the publisher's web-site:

Table S1. Sequence of each oligomer set for preparing genotype panel oligomers.

Table S2. Sequence of each genotype panel oligomers.

Table S3. Validation of our sample using current NAT system.

Table S4. Summary of DLC-chip analysis of genotype panels and international standards.

Online reporting system for transfusion-related adverse events to enhance recipient haemovigilance in Japan: A pilot study

Chikako Odaka[a], Hidefumi Kato[b], Hiroko Otsubo[a], Shigeru Takamoto[b], Yoshiaki Okada[a], Maiko Taneichi[a], Kazu Okuma[a], Kimitaka Sagawa[c], Yasutaka Hoshi[d], Tetsunori Tasaki[d], Yasuhiko Fujii[e], Yuji Yonemura[f], Noriaki Iwao[g], Asashi Tanaka[h], Hitoshi Okazaki[i], Shun-ya Momose[j], Junichi Kitazawa[k], Hiroshi Mori[l], Akio Matsushita[m], Hisako Nomura[n], Hitoshi Yasoshima[o], Yasushi Ohkusa[p], Kazunari Yamaguchi[a], Isao Hamaguchi[a,*]

[a] Department of Safety Research on Blood and Biological Products, National Institute of Infectious Diseases, Tokyo, Japan
[b] Department of Transfusion Medicine, Aichi Medical University, Aichi, Japan
[c] Department of Laboratory Medicine, Kurume University, Fukuoka, Japan
[d] Department of Transfusion Service, Tokyo Jikei University, Tokyo, Japan
[e] Department of Blood Transfusion, Yamaguchi University School of Medicine, Yamaguchi, Japan
[f] Department of Transfusion Medicine and Cell Therapy, Kumamoto University, Kumamoto, Japan
[g] Department of Transfusion Medicine and Cell Therapy, University of Yamanashi, Kumamoto, Japan
[h] Department of Blood Transfusion, Tokyo Medical University Hachioji Medical Center, Tokyo, Japan
[i] Central Blood Institute, Blood Service Headquarters, Japanese Red Cross Society, Tokyo, Japan
[j] Blood Service Headquarters, Japanese Red Cross Society, Tokyo, Japan
[k] Kuroishi General Hospital, Aomori, Japan
[l] Minami Tama Hospital, Tokyo, Japan
[m] Shibetsu City Hospital, Hokkaido, Japan
[n] Sanraku Hospital, Tokyo, Japan
[o] Yao General Hospital, Osaka, Japan
[p] Infectious Diseases Surveillance Center, National Institute of Infectious Diseases, Tokyo, Japan

ARTICLE INFO

ABSTRACT

Background: A surveillance system for transfusion-related adverse reactions and infectious diseases in Japan was started at a national level in 1993, but current reporting of events in recipients is performed on a voluntary basis. A reporting system which can collect information on all transfusion-related events in recipients is required in Japan.
Methods: We have developed an online reporting system for transfusion-related events and performed a pilot study in 12 hospitals from 2007 to 2010.
Results: The overall incidence of adverse events per transfusion bag was 1.47%. Platelet concentrates gave rise to statistically more adverse events (4.16%) than red blood cells (0.66%) and fresh-frozen plasma (0.93%). In addition, we found that the incidence of adverse events varied between hospitals according to their size and patient characteristics.
Conclusion: This online reporting system is useful for collection and analysis of actual adverse events in recipients of blood transfusions and may contribute to enhancement of the existing surveillance system for recipients in Japan.

© 2012 Published by Elsevier Ltd.

* Corresponding author. Address: Department of Safety Research on Blood and Biological Products, National Institute of Infectious Diseases, 4-7-1 Gakuen, Musashimurayama, Tokyo 208-0011, Japan. Tel.: +81 42 848 7120; fax: +81 42 567 2790.
E-mail address: 130hama@nih.go.jp (I. Hamaguchi).